

Changed Conformation of Mutant Tau-P301L Underlies the Moribund Tauopathy, Absent in Progressive, Nonlethal Axonopathy of Tau-4R/2N Transgenic Mice*

Received for publication, August 27, 2004, and in revised form, October 20, 2004
Published, JBC Papers in Press, October 27, 2004, DOI 10.1074/jbc.M409876200

Dick Terwel^{‡§}, Reena Lasrado^{‡§}, Johan Snauwaert^{‡¶}, Erno Vandeweer[¶],
Chris Van Haesendonck[¶], Peter Borghgraef[‡], and Fred Van Leuven^{‡¶}

From the [‡]Experimental Genetics Group, Department of Human Genetics, KU Leuven, B-3000 Leuven, Belgium and the [¶]Laboratory of Solid State Physics and Magnetism, KU Leuven, B-3001 Leuven, Belgium

Protein tau-3R/4R isoform ratio and phosphorylation regulates binding to microtubules and, when disturbed by aging or mutations, results in diverse tauopathies and in neurodegeneration. The underlying mechanisms were studied here in three transgenic mouse strains with identical genetic background, all expressing the tau-4R/2N isoform driven specifically in neurons by the *thy1* gene promoter. Two strains, expressing human tau-4R/2N or mutant tau-4R/2N-P301L at similar, moderate levels, developed very different phenotypes. Tau-4R/2N mice became motor-impaired already around age 6–8 weeks, accompanied by axonopathy (dilatations, spheroids), but no tau aggregates, and surviving normally. In contrast, tau-P301L mice developed neurofibrillary tangles from age 6 months, without axonal dilatations and, despite only minor motor problems, all succumbing before the age of 13 months. The third strain, obtained by tau knock-out/knock-in (tau-KOKI), expressed normal levels of wild-type human tau-4R/2N replacing all mouse tau isoforms. Tau-KOKI mice survived normally with minor motor problems late in life and without any obvious pathology. Biochemically, a fraction of neuronal tau in aging tau-P301L mice was hyperphosphorylated concomitant with conformational changes and aggregation, but overall, tau-4R/2N was actually more phosphorylated than tau-P301L. Significantly, tau with changed conformation and with hyperphosphorylation colocalized in the same neurons in aging tau-P301L mice. Taken together, we conclude that excessive binding of tau-4R/2N as opposed to reduced binding of tau-P301L to microtubules is responsible for the development of axonopathy and tauopathy, respectively, in tau-4R/2N and tau-P301L mice and that the conformational change of tau-P301L is a major determinant in triggering the tauopathy.

giving rise to very complex biochemical patterns (3–5). The only known function of tau is binding to microtubules to aid their initiation and stabilization, essential for axonal transport and thereby for synaptic integrity (reviewed in Ref. 6). Binding of tau to microtubules is dynamically regulated by phosphorylation and varying the isoform ratio tau-3R/4R (*i.e.* with three or four microtubule binding domains). Binding is affected by mutations associated with fronto-temporal dementia with parkinsonism linked to chromosome 17 (FTDP-17)¹. These comprise both amino acid substitutions, many located in exon 10 coding for the second microtubule binding domain, as well as intronic mutations that increase splicing-in of exon 10, to produce more tau-4R (3, 7–9).

Tauopathies are characterized by intracellular aggregates of tau that are invariably hyperphosphorylated, supporting the longstanding hypothesis that phosphorylation drives the process of self-aggregation. Remarkably, protein tau is a naturally unfolded protein that is very soluble and heat-stable but readily forms filaments *in vitro* and *in vivo* (10–14), whereas it is amazingly resistant to aggregation in transfected cells.

In vivo models are needed to define the patho-physiological repercussions of tau isoforms and mutants. Modeling tauopathy in terms of tau aggregation failed in transgenic mice expressing wild-type human tau (reviewed in Ref. 15). Our tau-4R/2N transgenic mice developed severe axonopathy due to axonal dilatations (spheroids) with Wallerian degeneration and severe motor problems but no tau aggregates (16). The axonopathy was fully corrected by co-expression of GSK-3 β , demonstrating for the first time *in vivo* that phosphorylation of tau is essential to prevent “clogging” of the axons (17), as in cells (18) by reducing binding of tau to microtubules. Expression of mutant tau in transgenic mice produced tau aggregates (19–22; reviewed in Ref. 15), demonstrating that tauopathy can be modeled in the short life span of mice. Alzheimer’s disease (AD) is the most common tauopathy and pathologically defined by extracellular amyloid plaques and neurofibrillary tangles (23). Mutant APP transgenic mice do not, however, develop tauopathy despite robust recapitulation of parenchymal and vascular amyloid pathology (reviewed in Refs. 19 and 24). Double transgenic mice, expressing mutant APP and mutant tau, combine amyloid and tau pathology but also amyotrophy and severe motor problems, atypical for AD (20, 25). Most recently, transgenic mice expressing three mutant human proteins (*i.e.* APP, PS1, and tau) displayed a combined amyloid and

The transcriptional and post-translational molecular heterogeneity of protein tau is extensive (reviewed in Refs. 1–3),

* This work was supported by Fonds voor Wetenschappelijk Onderzoek-Vlaanderen, the European Economic Community (EEC) 5th Framework Program, the Rooms-fund, the KU Leuven Research Fund and KU Leuven-R&D, the Instituut voor Aanmoediging van Wetenschappelijk en Technisch Onderzoek, the European Space Agency, and the EEC Marie Curie Training Site of the EURON Ph.D. School for Neurosciences. The costs of publication of this article were defrayed in part by the payment of page charges. This article must therefore be hereby marked “advertisement” in accordance with 18 U.S.C. Section 1734 solely to indicate this fact.

§ These authors contributed equally to this work.

¶ To whom correspondence should be addressed: Experimental Genetics Group-LEGT_EGG, Dept. Human Genetics, KU Leuven-Campus Gasthuisberg O&N 06, B-3000 Leuven, Belgium. Tel.: 32-16-34-58-88; Fax: 32-16-34-58-71; E-mail: fredvl@med.kuleuven.ac.be.

¹ The abbreviations used are: FTDP-17, fronto-temporal dementia with parkinsonism linked to chromosome 17; AD, Alzheimer’s disease; tau-KOKI, tau knock-out/knock-in; ES, embryonic stem; PBS, phosphate-buffered saline; TBS, Tris-buffered saline; CNS, central nervous system; mAb, monoclonal antibody.

TABLE I
Specifics of the primary antibodies against protein tau

Antibody	Epitope	Source, type	Reference
HT7	aa ^a 159–163, phosphorylation-independent	Innogenetics, mAb IgG1	53
Tau-5	Middle portion of tau, phosphorylation-independent	Pharmingen, mAb IgG1	54
AT8	Ser(P) ²⁰² /Thr(P) ²⁰⁵	Innogenetics, mAb IgG1	55
AT100	Thr(P) ²¹² /Ser(P) ²¹⁴	Innogenetics, mAb IgG1	50
AT180	Thr(P) ²³¹	Innogenetics, mAb IgG1	56
AT270	Thr(P) ¹⁸¹	Innogenetics, mAb IgG1	56
AD2	Ser(P) ³⁹⁶ /Ser(P) ⁴⁰⁴	A. Delacourte, mAb IgG1	57
AP422	Ser(P) ⁴²²	A. Delacourte, rabbit IgG	58
MC1	aa 5–15/312–322, conformation-dependent	P. Davies, mAb IgG1	38
TG3	Thr(P) ²³¹ /Ser(P) ²³⁵ , conformation-dependent	P. Davies, mAb IgM	59
PG5	Ser(P) ⁴⁰⁹	P. Davies, mAb IgG3	5

^a aa, amino acids.

tau pathology (26). Their behavioral and synaptic deficits appeared similar to those in APP and APP×PS1 transgenic mice (27–31), obscuring the exact contribution of the tau pathology.

The vast clinical heterogeneity of human tauopathies, even in the inherited cases, is due to different types of mutations as well as to genetic and epigenetic factors, since differences are even observed between patients with the same mutation in the same family (9). In sporadic tauopathies, more confounding factors must act (*i.e.* tau at different concentrations in different cell types; immunological, hormonal, and nutritional status; cholesterol and lipids; ApoE genotype; and more). This results in different clinical phenotypes, including or not including parkinsonism and motor and behavioral problems, and is reflected at the molecular level in different phosphorylation patterns of tau and in different morphology of tau filaments (paired helical, twisted, straight . . .). This baffling variability must and can be reduced in model systems to understand the basic molecular control mechanisms that underlie the physiological role of tau and the exact etiology in tauopathies.

To this end, we have generated and comprehensively phenotyped tau knock-out/wild-type tau-4R/2N knock-in mice (tau-KOKI) and tau-P301L transgenic mice and compared them to tau-4R/2N mice (16). Significantly, all three strains express the same tau-4R/2N isoform, with the P301L mutation in the tau-P301L mice at moderate levels from the same *thy1* gene promoter and all in the same genetic background. This strategy allowed us to separate the early, severe motor deficit in tau-4R/2N mice due to axonal dilations, but not tau aggregates, from the late minor motor impairment in tau-P301L mice, showing widespread intraneuronal tau aggregates and moribund neurodegeneration. This profound distinction is reflected at the molecular level by conformational changes of tau-P301L, not seen in wild-type tau-4R/2N.

EXPERIMENTAL PROCEDURES

Generation of Tau-P301L Transgenic Mice—The tau-4R/2N mice were generated and characterized previously (16, 17, 32). The same methods were used to generate transgenic mice expressing the longest human tau isoform with the P301L mutation (tau-4R/2N-P301L) under control of the same mouse *thy1* gene promoter (16, 27). Mutant tau-P301L was obtained by site-directed mutagenesis of tau-4R/2N and cloned into the blunted XhoI site of the *thy1* gene expression cassette. The construct was linearized with NotI and PvuI and injected into pre-nuclear mouse embryos (0.5-day) of the FVB/N strain. Embryos in the two-cell stage were transferred into the ampulla of synchronized foster CD1 or FVB/N female mice, and offspring were screened by PCR and Southern blotting of tail biopsy DNA according to standard procedures. The PCR primers for *thy1*-tau-P301L were 5'-CTGGGGCGGT-CAATAAT-3' and 5'-CAAGGTCCCGTTTCTCC-3'. The amplicon was used as probe in Southern blotting of genomic DNA, digested with StuI. The resulting four founders were mated, and offspring were genotyped and analyzed by Western blotting and by immunohistochemistry. Founder 2 with about 2-fold overexpression of tau-P301L transgene relative to endogenous tau was used for establishing a colony for further studies. Homozygous tau-P301L mice, obtained by inbreeding, were normally

fertile and transmitted the transgene stably to their offspring.

In this study, only homozygous tau-P301L mice were used in comparison with heterozygous tau-4R/2N mice (16), so as to have very comparable overall expression levels of respectively mutant and wild-type human tau-4R/2N in their brains.

Generation of Tau-KOKI Mice—The tau knock-out/knock-in strain of human wild-type tau-4R/2N (tau-KOKI) aimed to inactivate the endogenous murine tau gene and to replace it with a single copy of the *thy1*-tau-4R/2N recombinant DNA construct. This construct, previously used to generate tau-4R/2N mice (16), was linearized and ligated in a unique NcoI site in exon 1 of the mouse tau gene, partially subcloned from the 129 mouse strain (33). A 1.9-kb NotI fragment encoding the marker gene hygromycin B phosphotransferase driven by the phosphoglycerate kinase gene promoter was further ligated into a unique SmaI site. The targeting vector was linearized by NotI restriction and purified before electroporation into ES cells that were cultured in selective medium (hygromycin) and selected by standard procedures as described (34). Single colonies were expanded for genotyping using different probes including external and internal fragments of the murine and human tau gene and of the marker gene. ES cell colonies with the wanted homologous recombination were subcultured and genotyped before microinjection into 4-day-old blastocysts isolated from pregnant C57Bl/6 female mice. Reimplantation into pseudopregnant CD1 females by uterine transfer resulted in brown coat color chimeric mice proving germ line transmission of the ES cells. Offspring from the chimeras were crossed with FVB/N mice, and their offspring was analyzed by Southern blotting of tail DNA with the same probes described above. Heterozygous transgenic mice were mated to establish the tau-KOKI strain. The offspring was genotyped routinely at weaning by PCR on tail biop DNA. Breeding was continued by backcrossing into FVB/N for eight generations to obtain homozygous humanized tau-KOKI mice in the FVB/N background (*i.e.* the same background as that of the tau-4R/2N and tau-P301L mice). Homozygous and heterozygous tau-KOKI mice were differentiated by PCR with two sets of primers, one specific for the human tau-4R/2N cDNA and the other for exon 1 of the wild-type mouse tau gene.

Sensorimotor Tests—For the rod walking test, mice were placed in the middle of a 1.5-m-long horizontal rod (diameter 1.5 cm) and allowed a period of 3 min to remain and walk (score 1) or fall off (score 0) on a soft foam substrate. The automated rotarod test compared five mice at a time, placed on a revolving rod (diameter 3.2 cm between opaque side walls) (Med Associates, Georgia, VT). Subsequent to three learning trials on consecutive days (each 3 min at 20 rpm), mice were tested with the rod accelerating from 4 to 40 rpm in a 3-min time span. The time that the mice remained on the revolving rod was logged automatically. Data on rotarod performance were analyzed by two-way analysis of variance with genotype and age as independent variables and time on the rod as dependent variable. Data were further analyzed by one-way analysis of variance with age or strain as the independent variable and time on the rod as the dependent variable, followed by Student-Newman-Keuls *post hoc* multiple comparison (set at $p < 0.05$). Statistical evaluation of differences in the risk of falling off of the beam between wild-type and transgenic mice was performed by the corrected χ^2 test, with associated two-sided p values determined.

Antibodies—The specifications of antibodies against phosphorylation-independent, phosphorylation-dependent, and conformational epitopes of protein tau used in the present studies are summarized in Table I. In addition, SMI-32 antibody directed against nonphosphorylated neurofilament H (Sternberger, Lutherville, MD) was used to detect axonal dilations (16, 17).

Immunohistochemistry—Mice were anesthetized with pentobarbital (120 mg/kg, intraperitoneally), flushed by transcardiac perfusion with ice-cold saline (2 ml/min for 2 min), and fixed with 4% paraformaldehyde in PBS (2 ml/min for 10 min). Brain and spinal cord were removed, postfixed overnight in 4% paraformaldehyde in PBS, and stored in 0.1% sodium azide in PBS at 4 °C. Coronal and saggital 40- μ m-thick sections were cut, rinsed in PBS, and treated with 1.5% H₂O₂, 50% methanol in PBS. Nonspecific binding of antibodies was blocked by treatment with 10% fetal calf serum, 3% bovine serum albumin in PBS (blocking buffer). The sections were incubated with primary antibody in blocking buffer (with 0.1% Triton X-100) at ambient temperature overnight. Dilutions of the primary antibodies used (and method of amplification) were as follows: HT7, 1:10,000 (two-step); AT8, 1:1000 (two-step and three-step); AT180, 1:250 (two-step); AT270, 1:5000 (two-step); AD2, 1:1000 (two-step); AT100, 1:1000 (two-step) or 1:5000 (three-step); AP422, 1:1000 (two-step); MC1, 1:1000 (two-step and three-step).

The sections were then incubated for 1 h with goat anti-mouse or anti-rabbit IgG-horseradish peroxidase (two-step procedure) or goat anti-mouse or anti-rabbit IgG-biotin (three-step procedure), diluted 1:500 in blocking buffer, 0.1% Triton X-100. In the two-step procedure, the sections were next washed with PBS and 50 mM Tris-HCl (pH 7.6) for 5 min and stained with 3,3'-diaminobenzidine, 0.3% H₂O₂ in 50 mM Tris-HCl (pH 7.6) for 3–5 min. In the three-step procedure, the sections were incubated with avidin-biotinylated peroxidase complex (Vectastain Elite ABC, Vector, Burlingame, CA) diluted 1:800 in PBS, 0.3% bovine serum albumin for 1 h at ambient temperature and sometimes briefly counterstained with hematoxylin, as indicated. Finally, the sections were washed and stained as in the two-step procedure. Sections were dehydrated by passage through a graded series of alcohol and xylol and mounted.

Except where otherwise indicated, double immunolabeling was performed similarly, with sections incubated with primary antibodies in the following dilutions: AP422 and HT7, 1:1000; AT8, AT100, and MC1, 1:500. Sections were incubated with secondary antibodies goat anti-rabbit IgG-horseradish peroxidase-labeled and goat anti-mouse IgG-alkaline phosphatase labeled and developed with aminoethylcarbazole or with nitro blue tetrazolium as substrates. The sections were mounted on silanized slides in Kaiser's glycerol gelatin.

Histology—Silver impregnation of brain sections was exactly as described (35). For staining with thioflavin S, sections were washed twice for 1 min in water and incubated with 1% thioflavin S in water for 8 min, washed and refixed with 4% formaldehyde for 10 min, rinsed in water for 1 min, and incubated again with 1% thioflavin S for 4 min. Excess thioflavin S was removed by washing with 80% ethanol twice for 1 min each. Finally, the sections were mounted in 10% Mowiol, 25% glycerol, 100 mM Tris-HCl (pH 8.5), 40 mg/ml triethylenediamine. Staining with X-34, a derivative of Congo Red that stains β -pleated proteins, was carried out essentially as described (36). Sections were washed twice for 2 min in PBS and incubated in 0.1 mM X-34 in 40% ethanol. Sections were rinsed five times in tap water and treated with 0.2% NaOH in 80% ethanol. The sections were washed twice for 5 min in water before mounting in 10% Mowiol, 25% glycerol, 100 mM Tris-HCl (pH 8.5), 40 mg/ml triethylenediamine.

Brain Tissue Extracts—Brain tissue was homogenized in 6 volumes of buffer. The homogenate was centrifuged at 150,000 \times g for 30 min, and the supernatant was stored at -70 °C in aliquots. The pellet was resuspended in 6 volumes of 10 mM Tris-HCl (pH 7.6), 0.8 M NaCl, 10% sucrose, 1 mM phenylmethylsulfonyl fluoride and again centrifuged at 20,000 \times g for 30 min. The supernatant was made 1% in Sarkosyl and incubated for 1 h at room temperature before centrifugation at 150,000 \times g for 30 min. The pellet comprising the Sarkosyl-insoluble material was resuspended in TBS.

Western Blotting—Mice were killed by decapitation, brain was removed from the skull and spinal cord from the chorda, and tissues were snap-frozen in liquid nitrogen. Brain and spinal cord were homogenized in 6 volumes of homogenization buffer (25 mM Tris-HCl (pH 7.6), 150 mM NaCl, 1 mM EDTA, 1 mM EGTA, 5 mM sodium pyrophosphate, 30 mM sodium fluoride, 2 mM sodium vanadate, 1 μ M okadaic acid, 1 mM phenylmethylsulfonyl fluoride, 5 μ g/ml leupeptin, 5 μ g/ml pepstatin, 5 μ g/ml soy bean trypsin inhibitor) in a Potter-Elvehjem homogenizer with 20 up-and-down strokes of a Teflon pestle rotating at 700 rpm. Brain and spinal cord homogenates were diluted appropriately in sample buffer for SDS-PAGE on 8% polyacrylamide gels (Novex, San Diego, CA). Proteins were transferred to nitrocellulose filters (Hybond-ECL) at 70 mA overnight, in 25 mM Tris-HCl (pH 8.6), 190 mM glycine, 20% methanol. Filters were stained with Ponceau Red to visualize proteins as loading control and washed three times in 50 mM Tris-HCl (pH 7.6), 150 mM NaCl, 0.1% Tween (TBS-Tween) for 10 min. To prevent nonspecific binding of anti-

body, the blots were blocked by 5% nonfatty milk in TBS-Tween. The blots were incubated at 4 °C for 2 h with the primary antibody diluted in the same buffer. The dilutions of the primary antibodies were as follows: Tau-5, 1:1000; AT8, 1:200; AT180, 1:200; AT100, 1:200; AT270, 1:500; AD2, 1:5000. Primary antibody was removed by washing four times with TBS-Tween for 8 min. Blots were incubated for 1 h with labeled secondary antibody (goat anti-mouse or anti-rabbit IgG-horseradish peroxidase, 1:10,000; Bio-Rad), and reactions were visualized by ECL (Amersham Biosciences).

Immunogold Electron Microscopy—Sarkosyl insoluble fractions were applied on 200-mesh Formvar carbon-coated nickel grids in drops of 5 μ l and allowed to air-dry overnight. Grids were incubated with diluted primary antibody in PBS, 0.1% gelatin (cold water fish) for 90 min at room temperature. Primary antibody dilutions were as follows: HT7, 1:50; AT8, 1:50; AT100, 1:50; MC1, 1:2; TG3, 1:2. Grids were washed in 0.1% cold water fish gelatin and incubated with secondary antibody (goat anti-mouse IgG/M) labeled with 10-nm gold particles (Aurion) diluted 1:30 in PBS, 1% cold water fish gelatin. After washing in PBS, tau filaments were negatively stained with 2% uranyl acetate for 5 min. After air drying, the grids were examined by transmission electron microscopy (Philips CM10) at 80 kV, and images were obtained at magnifications of \times 52,000 and \times 105,000.

Atomic Force Microscopy—Tau filaments resuspended in TBS were deposited on silanized silicon supports and washed twice with distilled water before analysis by atomic force microscopy in tapping mode on the Nanoscope III (Digital Instruments, Santa Barbara, CA) equipped with a SuperSharpSilicon™ cantilever (Nanoworld AG, Neuchatel, Switzerland).

RESULTS

Generation of Tau-KOKI Mice and Tau-P301L Mice—To generate transgenic mice that lack the heterogeneity of the six tau isoforms due to alternative RNA splicing, we inactivated the endogenous tau gene by introducing into exon 1 a single copy of the human tau-4R/2N cDNA under control of the mouse *thy1* promoter. This construct was based on the same cassette used to generate the tau-4R/2N mice (16), now incorporated into a genomic DNA fragment containing the first exon of the mouse tau gene (33). Standard methods of homologous recombination in ES cells and of analysis by Southern blotting of 336 independent ES clones yielded six ES clones that had undergone correct homologous recombination (results not shown). One ES cell line yielded germ line chimeras that were mated to FVB mice, and the F1 offspring were back-crossed for eight generations into the FVB strain before crossing to yield homozygous tau-KOKI mice, analyzed here.

In the tau-KOKI mice, mouse tau was completely lacking, whereas neuronal expression of the human tau-4R/2N transgene was biochemically demonstrated to begin in the second week after birth, similar to other transgenes driven by the same mouse *thy1* gene promoter (16, 17, 27). This independently demonstrates that the impact of the absence of endogenous mouse tau on the developing mouse embryo is practically negligible (33), indicating that its function is taken over by other microtubule-associated proteins. Phenotypically, until the age of about 6 months, homozygous tau-KOKI mice were indistinguishable from wild-type mice, with normal body weight, normal behavior in the home cage, normal rearing and grooming, and normal fertility with normal frequency and size of litters.

In parallel, we generated tau-4R/2N-P301L mice in which the P301L FTDP-17 mutation was introduced by site-directed mutagenesis in the tau-4R/2N isoform cloned in the mouse *thy1* gene promoter cassette and microinjected as described (16, 27). Three independent founder strains of tau-P301L mice were compared for expression of human tau by Western blotting and by immunohistochemistry. Offspring of all three founders expressed human protein tau in neurons in layers II, V, and VI of the neocortex, in layer III of the entorhinal cortex, in the basolateral amygdala, hippocampus, zona incerta of the thalamus, brain stem nuclei, deep cerebellar nuclei, and spinal cord

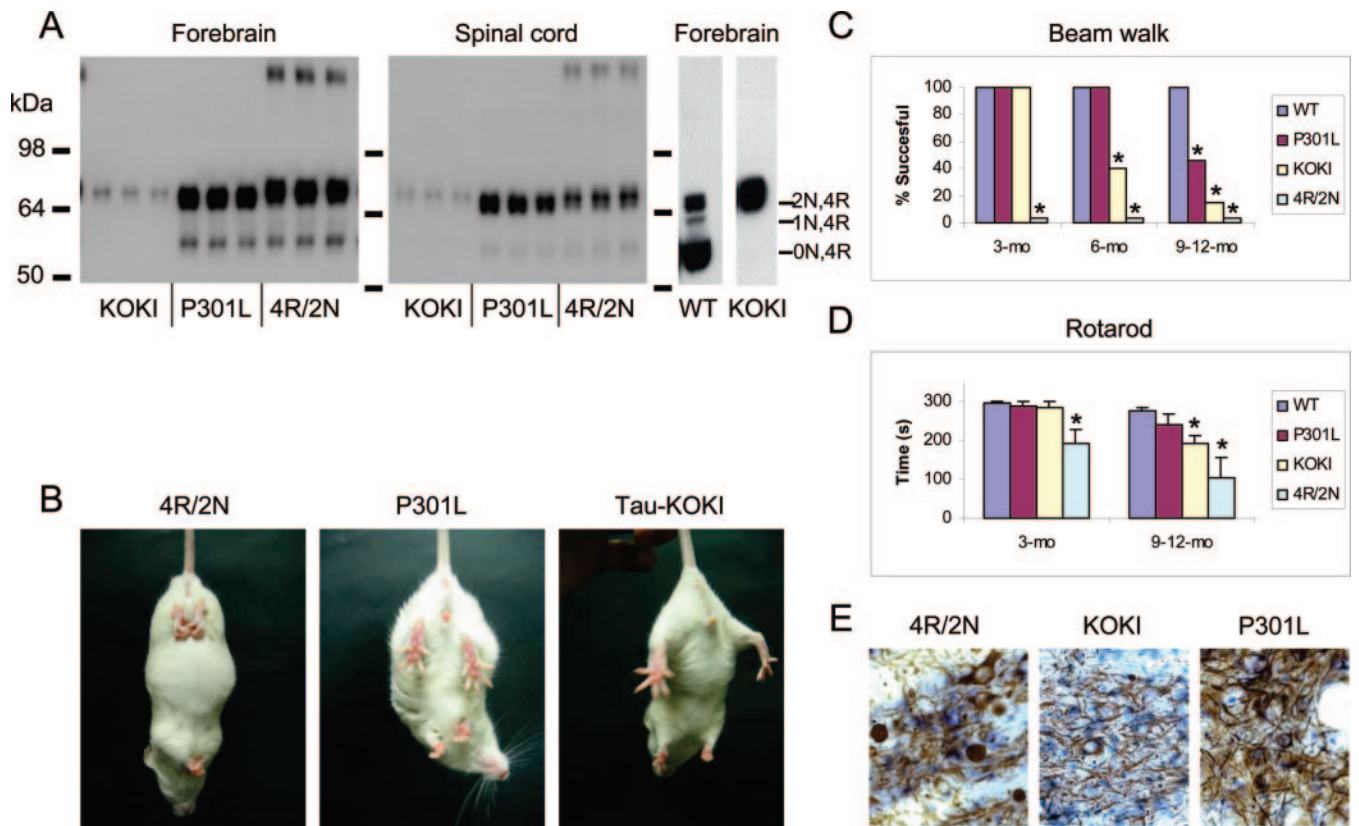


FIG. 1. Major characteristics of tau-KOKI, tau-P301L, and tau-4R/2N mice. *A*, Western blotting with mAb Tau-5 defines the level of protein tau in brain and spinal cord of three mice with each of the genotypes specified. Apparent molecular mass is indicated in kDa on the left. Approximate positions of major isoforms of tau-4R with 0, 1, and 2 N-terminal inserts (0N, 4R; 1N, 4R; and 2N, 4R) are indicated on the right. Different exposure times were used to highlight the major issues as discussed throughout. The high molecular weight bands are typical in tau-4R/2N mice and represent dimers of tau-4R/2N (16). *B*, typical clasping of the limbs when lifted by the tail is much less severe in tau-P301L mice, showing only partial retraction and still spreading of toes, as opposed to tau-4R/2N mice. Tau-KOKI never showed clasping even when very old. Mice depicted were 9 months. *C*, beam walk test of wild-type (WT), tau-P301L, tau-KOKI, and tau-4R/2N mice at the specified ages. Values represent the number of mice that succeeded in staying on the beam for 3 min (yes or no score). The number of mice analyzed were as follows: at 3 months, $n = 15, 6, 10, \text{ and } 8$; at 6 months, $n = 15, 8, 10, \text{ and } 3$; at 9–12 months, $n = 18, 11, 10, \text{ and } 8$, respectively, for the four genotypes specified. The asterisks denote significant difference with respect to age-matched nontransgenic mice ($p < 0.01$). *D*, Rotarod test of wild-type, tau-P301L, tau-KOKI, and tau-4R/2N mice at the specified ages. Values represent the time spent on the rotating rod (mean \pm S.E.). The number of mice analyzed was as follows: at 3 months, $n = 9, 8, 10, \text{ and } 5$; at 9–12 months, $n = 10, 9, 10, \text{ and } 5$, respectively, for the four genotypes specified. The asterisks denote significant difference with respect to age-matched nontransgenic mice ($p < 0.05$). *E*, immunohistochemistry with SMI-32 on sagittal sections of trigeminal nucleus of 3-month-old mice of the specified genotypes (original magnification $\times 40$). Note the axonal dilations or spheroids in tau-4R/2N mice, completely absent in tau-KOKI and tau-P301L mice.

(results not shown). Strain 2 was selected for experiments because the expression of human tau-P301L was robust in neurons throughout the central nervous system (CNS), including spinal cord and thereby quantitatively and qualitatively similar to the tau-4R/2N mice as characterized before (16).

Important to note is that all three mouse strains expressed the human tau-4R/2N isoform, evidently containing the mutation in the tau-P301L mice. Moreover, all transgenes are under control of the mouse *thy1* gene promoter, and all mice have the identical pure FVB genetic background. This strict strategy warranted that the temporal and regional and neuron-specific expression throughout the CNS was similar in all three mouse strains. In all experiments reported here, we analyzed heterozygous tau-4R/2N mice and homozygous tau-P301L mice that have very comparable concentrations of human tau in their brain and spinal cord at moderate overexpression levels (*i.e.* about 4-fold higher than endogenous mouse protein tau) (Fig. 1A). Therefore, the only difference between the tau-4R/2N and tau-P301L mice is the presence of the P301L mutation, whereas the only difference between the tau-4R/2N and tau-KOKI mice is the level of expression (*i.e.* endogenous and 4-fold increased, respectively).

The tau-KOKI mice were bred homozygous for the recombinant tau-locus so as to have expression of human tau-4R/2N

only, and at levels that were similar to those of endogenous mouse tau in nontransgenic mice, but evidently without the isoform variety (Fig. 1A, right). mAb Tau-5 reacts with all human and mouse tau isoforms independent of their phosphorylation status and was used to estimate the total level of tau at about 4 times higher in tau-4R/2N and tau-P301L mice than in the tau-KOKI mice (Fig. 1A).

Tau-4R/2N but Not Tau-P301L Caused Severe Motor Impairment and Axonopathy—The most conspicuous phenotypic aspect of tau-4R/2N mice was their severe motor defect, first observed as clasping, by caretakers in the home cages (Fig. 1B) (16). The motoric deficit developed early in life (*i.e.* at about 6–8 weeks in heterozygous tau-4R/2N mice) and is caused by a progressing axonopathy, typified by numerous axonal dilations (spheroids) in brain and spinal cord, followed by Wallerian degeneration and muscle wasting as studied extensively before (16).

Only old tau-P301L mice (9–12 months) typically retracted their hind limbs, and only some retracted all four limbs (Fig. 1B). This clasping occurred later in life and was different and less severe than in tau-4R/2N mice, which displayed this simple but clear phenotypic trait already at age 6–8 weeks (Fig. 1B) (16). No motor problems were observed before age 6 months in tau-P301L mice when minor paresis of the hind limbs began

to appear in some mice. This progressed with age in all tau-P301L mice to include also the forelimbs, so that around age 9–10 months, most tau-P301L mice showed moderate to severe decline in ambulation in the home cage. They began to lose weight due to muscle and tissue wasting, and this moribund condition was terminal for all homozygous tau-P301L mice at 11–13 months of age. The direct cause of death could not be determined on necropsy, nor by examination of old, terminally ill tau-P301L mice. Since only neurons express the transgene, but in all regions of the CNS, widespread neurodegeneration must be retained as the prime candidate.

The pronounced difference and age dependence of the motor deficit were measured by two objective tests (*i.e.* beam-walking and rotarod). Both tests unequivocally confirmed that the original tau-4R/2N mice were the most early and the most severely affected; no tau-4R/2N mouse was able to stay on the beam even at 3 months of age (Fig. 1C). Also on the rotarod, tau-4R/2N mice performed worst both at 3 and 9 months of age (Fig. 1D). This contrasted sharply with the nearly normal rotarod performance of the tau-P301L mice; neither at 3 nor at 9–12 months were tau-P301L mice significantly impaired, neither during acquisition (not shown) nor in the final test (Fig. 1D). This clear difference between tau-4R/2N and tau-P301L mice was confirmed by the beam walk test at 3 and 6 months of age, revealing a deficit only in some of the oldest tau-P301L mice (Fig. 1C). Both tests objectively extended the simple clasping test to demonstrate the pronounced difference in phenotypic repercussions of the mutant tau-4R/2N-P301L relative to the tau-4R/2N transgene.

The tau-KOKI mice did not show limb clasping when lifted by the tail at any age, even when very old (2 years) (Fig. 1B). Nevertheless, tau-KOKI mice of 9–12 months were impaired in rotarod performance (Fig. 1D), whereas almost all tau-KOKI mice of 9–12 months and many already at 6 months failed the beam walk test (Fig. 1B).

These marked exterior phenotypic differences were underlined by the pathological analysis of brain and spinal cord. The widespread abundance of axonal dilatations in the brain and spinal cord of tau-4R/2N mice was again evident (Fig. 1E) (16). On the contrary, axonal dilatations were completely absent in brain and spinal cord of tau-P301L mice at any age (3, 6, and 9–12 months, $n = 6$ each), even when terminally ill. Likewise, axonal dilatations were never observed in tau-KOKI mice ($n = 32$; analyzed at different ages, including eight mice of 18–20 months). Quantitative analysis of axonal dilatations in the trigeminal nucleus of tau-4R/2N mice at 3 months of age amounted to 25 ± 5 dilatations/mm² (mean \pm S.E., $n = 3$), whereas in aged-matched tau-KOKI and tau-P301L mice, no dilatations were present.

The combined data demonstrate that the severe motor deficit of the tau-4R/2N mice was related to the higher level of tau-4R/2N, whereas remarkably, even normal levels of tau-4R/2N in the tau-KOKI mice resulted in a motor deficit that was more pronounced than in tau-P301L mice. This can be due to the absence of the tau-3R isoforms but is more likely due to the fact that the level of tau-4R/2N is higher than in the brain of nontransgenic mice (Fig. 1, C and D), and, moreover, tau is present only in neurons due to the use of the *thyl* gene promoter. The evident gene-dosage effect earmarks the wild-type human tau-4R/2N isoform as the cause of the motor deficit, itself manifested by the axonal dilatations (16) that are due to “clogging” of the axons by the excessive binding of tau-4R/2N to microtubules (17, 18). The P301L mutation prevented the tau-4R/2N isoform to cause axonal dilatations and to a large extent the motor deficit, most likely by its lesser affinity for binding to microtubules (37) allowing normal axonal transport (6).

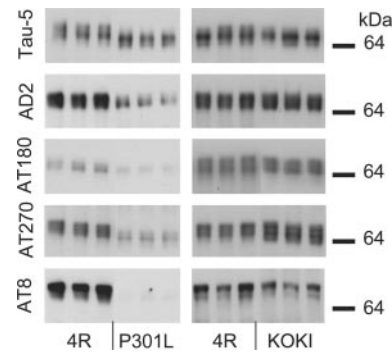


FIG. 2. Phosphorylation of tau in brain of tau-4R/2N, tau-P301L, and tau-KOKI mice. Shown is Western blotting for the phosphorylation-dependent epitopes specified, in extracts from three individual mice at age 3 months with the specified genotypes. For blotting with tau-5, AD2, and AT270, the equivalent of 0.4 μ g of brain protein was loaded per lane, whereas 4 μ g was loaded for detection with AT8 and AT180. For the tau-KOKI mice, 4 times more protein was loaded per lane. Different exposure times were used for the different antibodies. Apparent molecular mass is indicated on the right in kDa.

Clearly, axonal dilatations are not a prerequisite for the mild motor deficit in either tau-KOKI or tau-P301L mice, but are the externalization of the severe axonopathy in tau-4R/2N mice. It is envisaged that at lower expression levels, tau-4R/2N impairs transport in the longer axons of motor neurons, causing motor problems without axonal dilatations. In fact, even in tau-4R/2N mice, the vast majority of neurons have normal axons and no dilatations. In the tau-P301L mice, the motor neurons probably become functionally impaired due to the aggregates of tau that eventually cause the minor motor impairment, as described and discussed further.

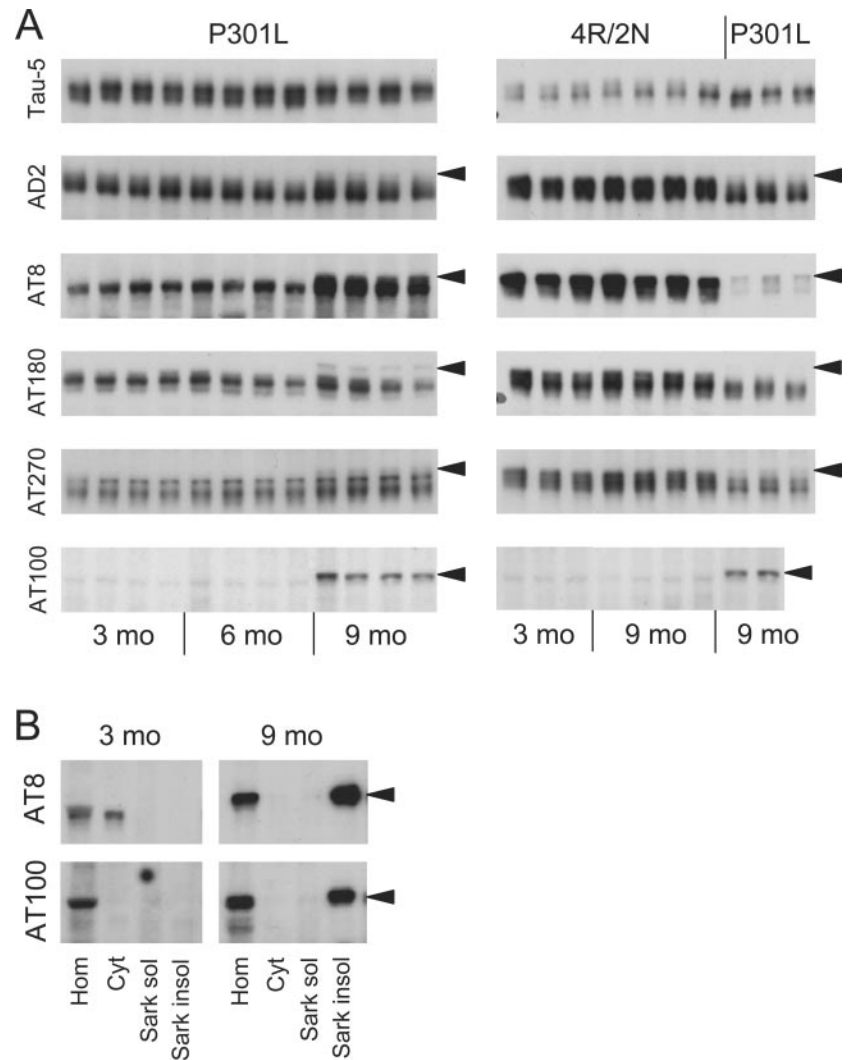
Tau-4R/2N Is More Phosphorylated than Tau-P301L in Brains of Young Mice—Since the affinity of tau for microtubules depends on its phosphorylation, the brains of mice of the three genotypes were analyzed biochemically with antibodies specific for relevant phosphorylation sites on tau. We compared different groups of individual tau-KOKI and tau-P301L mice each to age-matched tau-4R/2N mice (representative analysis of three mice at age 3 months is shown in Fig. 2). Total levels of tau were determined by Western blotting with mAb Tau-5 that defines a stable epitope not affected by phosphorylation. This made already clear that the overall electrophoretic mobility of tau-4R/2N was slower than that of tau-P301L (Fig. 2, upper left; see also Fig. 1A), which must be attributed to post-translational modifications, mainly phosphorylation.

All phosphorylation-dependent epitopes were detected in all mice, but the brains of tau-P301L mice contained consistently less phosphorylated tau at 3 months of age than age-matched tau-4R/2N mice (Fig. 2, left). This was most conspicuous for AT8 and AT180 epitopes (Fig. 2), whereas no immunoreactivity was observed by Western blotting with mAb AT100, defining a typical disease-associated epitope, in brain extracts of young mice of any genotype at 3 months of age.

For comparison of tau-KOKI with tau-4R/2N mice, 4 times more brain protein extract was loaded from the tau-KOKI mice to compensate for the lower expression of tau-4R/2N (Fig. 2, right; compare also with Fig. 1A). No marked differences were observed in reaction with any of the mAbs (Fig. 2, right), demonstrating that the relative phosphorylation of tau-4R/2N in the tau-KOKI mice was very similar to that in the tau-4R/2N mice when normalized for the difference in expression.

Tau-P301L but Not Tau-4R/2N Becomes Hyperphosphorylated and Sarkosyl-insoluble with Aging—Since, somewhat unexpectedly, tau-P301L appeared underphosphorylated at a young age, we analyzed biochemically in more detail the progression and the distribution of phosphorylated tau with age.

FIG. 3. Progression with age of phosphorylation-dependent epitopes in brain of tau-P301L and tau-4R/2N mice. A, Western blotting of brain extracts from tau-P301L mice (*right*) and tau-4R/2N mice (*left*) with Tau-5, AD2, AT8, AT180, AT270, and AT100. The equivalent of 0.4 μ g of protein was loaded per lane for detection with Tau-5, AD2, and AT270, whereas 4 μ g was loaded for detection with AT8, AT100, and AT180. Shown are data for four and 3–4 individual tau-P301L and tau-4R/2N mice, respectively, for each specified age. Since results for the *left* and *right* panels were not obtained at the same time, samples for 9-month-old tau-P301L mice were loaded twice for reference. B, Western blotting with AT8 and AT100 of the specified fractions isolated from spinal cords of tau-P301L mice 3 and 9 months old. For homogenate, cytosol, Sarkosyl-soluble, and Sarkosyl-insoluble fraction, 36, 36, 14.4, and 36 μ g, respectively, of the original tissue weight was loaded per lane. In both panels, the arrowheads indicate the position of the hyperphosphorylated tau referred to throughout.



The progressive phosphorylation of tau with age was analyzed by Western blotting with a panel of monoclonal antibodies on total homogenates of brain from individual mice of each genotype at 3, 6, and 9 months of age. Surprisingly, aging affected phosphorylation of tau mainly in the tau-P301L mice, both in the brain and spinal cord (Fig. 3A, *left*), whereas practically no changes were observed in tau-4R/2N (Fig. 3, A (*right*) and B, and results not shown) and tau-KOKI mice within this time frame (results not shown). Besides the distinct increased AT8 reactivity, the very prominent appearance of the AT100 epitope was conspicuous in brain of all old tau-P301L mice (>9 months) (Fig. 3A). The AT100 epitope was carried largely by the slowest migrating tau subspecies that also carried AT8 and to a lesser extent AT180, AT270, and AD2 epitopes (Fig. 3A, *arrowheads*).

Fractionation of the CNS of tau-P301L mice demonstrated that mainly the Sarkosyl-insoluble fractions were enriched in phosphoepitopes and that AT8 and AT100 epitopes appeared nearly exclusively in this fraction (Fig. 3B). Since these epitopes are very typical and pathologically carried by tau present in paired helical filaments and neurofibrillary tangles, we further extended the fractionation analysis.

Cytosol and Sarkosyl-soluble and -insoluble fractions were prepared from brains of tau-P301L, tau-4R/2N, and tau-KOKI mice and spinal cord of tau-P301L and tau-4R/2N mice, all age-matched at 3 and 9 months. The level of human tau in the fractions was defined by Western blotting with mAb HT7 that is specific for human tau (Fig. 4). Besides tau, an unknown protein was detected with HT7 mainly in the Sarkosyl-soluble

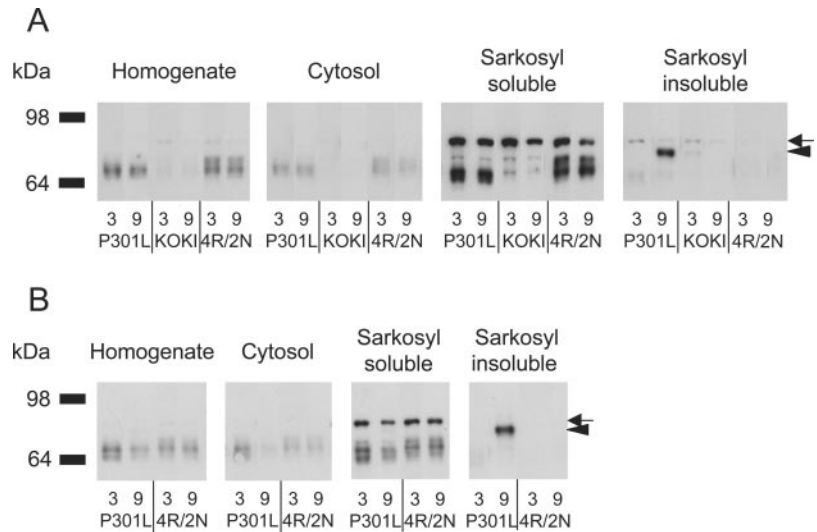
fraction in all mice, independent of age and genotype (Fig. 4A, *large arrow*). Since this protein was not detected with Tau-5 or with any of the other mAbs, it is neither human nor mouse protein tau and was not considered further.

Most conspicuous were the electrophoretically slow tau forms detected in the Sarkosyl-insoluble fraction from the spinal cords (Fig. 4B) and from the brains (Fig. 4A, *arrowhead*) of old tau-P301L mice, which were immunohistochemically shown to contain neurofibrillary tangles (see below). These tau species were never observed in extracts of tau-4R/2N and tau-KOKI mice (Fig. 4, A and B) and are therefore the biochemical equivalent of the aggregated tau in tangle-bearing neurons.

The close similarity of the pattern in fractions of brain and spinal cord of tau-4R/2N and tau-P301L mice also demonstrates that functionally widely divergent neurons in different regions of the CNS reacted similarly but distinctively to each transgene. This is an important finding, since it demonstrates that the molecular characteristics of each tau species (tau-4R/2N and tau-P301L) are actually the major determinants for each distinctive response (axonopathy or tauopathy).

Pathological Epitopes on Tau-P301L but Not on Tau-4R/2N Accumulate in Somata in Old Mice—Mice of all genotypes were analyzed immunohistochemically for tau phosphoepitopes. In both tau-4R/2N and tau-P301L mice, immunoreactivity with AT180, AT270, and AD2 was present in neurons in brain and spinal cord in a pattern similar to that with HT7, but less intense and mainly confined to the somatodendritic compartment (results not shown).

FIG. 4. Fractionation of brain and spinal cord of tau-P301L, tau-KOKI, and tau-4R/2N mice. Shown is Western blotting with human tau-specific mAb HT7 of the specified fractions of brain (A) and spinal cord (B) from mice with the specified genotype at 3 and 9 months of age, as indicated. Different amounts of homogenate, cytosol, Sarkosyl-soluble fraction, and Sarkosyl-insoluble fraction were loaded of forebrain (*i.e.* 3.6-, 3.6-, 14.4-, and 72- μ g equivalents, respectively) of the original brain weight per lane. For spinal cord, identical amounts were loaded. Apparent molecular mass is indicated on the left in kDa. In A, the arrow points to the unidentified cross-reacting protein in the Sarkosyl-soluble fraction also present in the equivalent spinal cord fraction. The arrowhead points to the slowest migrating tau species in the Sarkosyl-insoluble fraction.



mAb AT8 highlighted the most marked difference between tau-4R/2N and tau-P301L mice, staining mainly the neuropil in tau-4R/2N mice (Fig. 5A, *e* and *f*) as opposed to the somatodendritic compartments of neurons in tau-P301L mice (Fig. 5A, *c* and *d*). In old tau-P301L mice, reactivity with AT8 and also AD2 was more intense in neurons scattered throughout the cortex and the zona incerta of the thalamus, in brain stem, in deep nuclei of the cerebellum, and in spinal cord. This was observed already in some tau-P301L mice at 6 months of age while prominent in all old tau-P301L mice (Fig. 5A).

The pathological AT100, AP422, and PG5 epitopes were also confined mainly to the neuronal soma of all old tau-P301L mice, while detectable also in some 6-month-old tau-P301L mice (Fig. 5B, *a-d*).

Reaction with AT100, AP422, and PG5 was completely absent in tau-4R/2N mice (Fig. 5B, *e* and *f*, and results not shown), whereas none of the antibodies reacted appreciably with brain or spinal cord from tau-KOKI mice or from nontransgenic mice (results not shown).

The histochemical analysis extends the biochemical data on hyperphosphorylated tau accumulation in tau-P301L mice and not in tau-4R/2N mice, with the extra information on the subcellular localization (*i.e.* concentration into the somatodendritic compartments within the brain of old tau-P301L mice). This is completely in line with observations of neurofibrillary tangles in neuronal soma in human tauopathies.

Tauopathy and Conformational Epitopes Characterize Tau-P301L Mice and Are Absent in Tau-4R/2N Mice—Neurofibrillary pathology was evident in all old tau-P301L mice by silver impregnation (Fig. 6A, *d* and *e*) and fluorescent staining with thioflavin S and X-34 (Fig. 6A, *a* and *c*) (36). Positive neurons were abundant in brain and spinal cord of all tau-P301L mice of 9 months and older and absent or weak in CNS of younger tau-P301L mice. Reaction with thioflavin S or X-34 was completely absent from CNS of tau-KOKI mice or tau-4R/2N mice even when very old (22–30 months) (results not shown), confirming the total absence of tauopathy in tau-4R/2N mice (16).

The tauopathy in old tau-P301L mice was also visualized with AT8 (Figs. 5A and 6A, *f1*), showing immunoreactivity in soma, proximal dendrites, and dendritic branches and spines of affected neurons. Remarkably, AT8 immunoreactivity in younger tau-P301L animals was present in fine granules, whereas in older animals also large, intensely staining granules and clusters were evident (Fig. 6A, *f2*). These clusters and granules were also argyrophilic, although this reaction was more confined to proximal dendrites and somata (Fig. 6A, *d* and *e*).

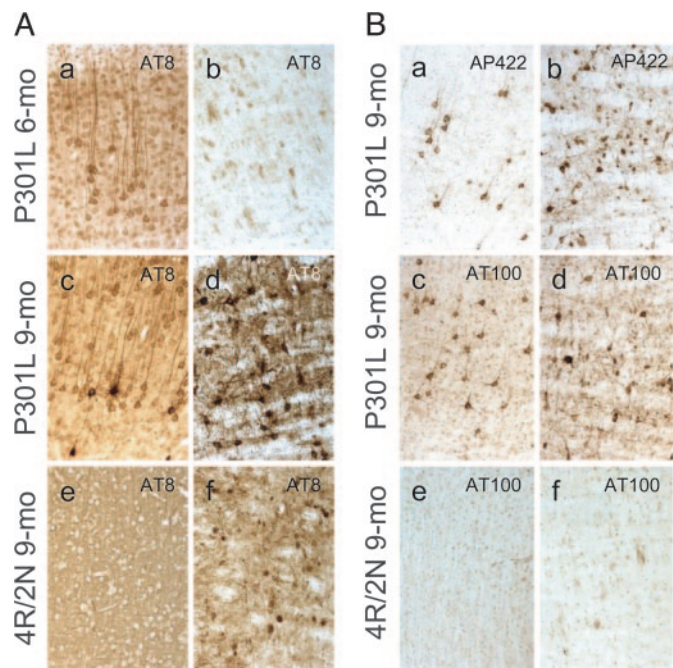


FIG. 5. Somatodendritic relocation of hyperphosphorylated tau in tau-P301L mice with age. A, AT8-immunoreactive neurons in cortex (*a*, *c*, and *e*) and brain stem (*b*, *d*, and *f*) of tau-P301L mice at 6 months (*a* and *b*) and 9 months (*c* and *d*) and of tau-4R/2N mouse at 9 months (*e* and *f*). B, AP422 (*a* and *b*) and AT100 (*c-f*) immunoreactive neurons in cortex (*a*, *c*, and *e*) and brain stem (*b*, *d*, and *f*) of tau-P301L mouse (*a-d*) and tau-4R/2N mouse (*e* and *f*) at 9 months of age. Sagittal sections were used. Original magnifications were $\times 40$.

Besides the pathological AP422 and AT100 epitopes (Fig. 5B, *a-d*), also the conformational epitopes defined by MC1 and TG3 were ominously present in brain of tau-P301L (Fig. 7). mAb MC1 defines a complex, nonlinear epitope combining the N terminus of tau with the microtubule binding domain (38). The MC1 reaction was observed in CNS of all old tau-P301L mice (Fig. 7, A, D, and E), whereas it was absent or rare in 6-month-old tau-P301L mice and totally absent in CNS of tau-4R/2N, nontransgenic, and tau-KOKI mice at any age (up to 24 months) (Fig. 7, B and C, and results not shown). Significantly, MC1-immunoreactive neurons were present in similar numbers and distributed like AT100-, AP422-, and PG5-reactive neurons (compare Fig. 5B, *a-d*, with Fig. 7, D and E). The extent of correlation was illustrated by double labeling with the

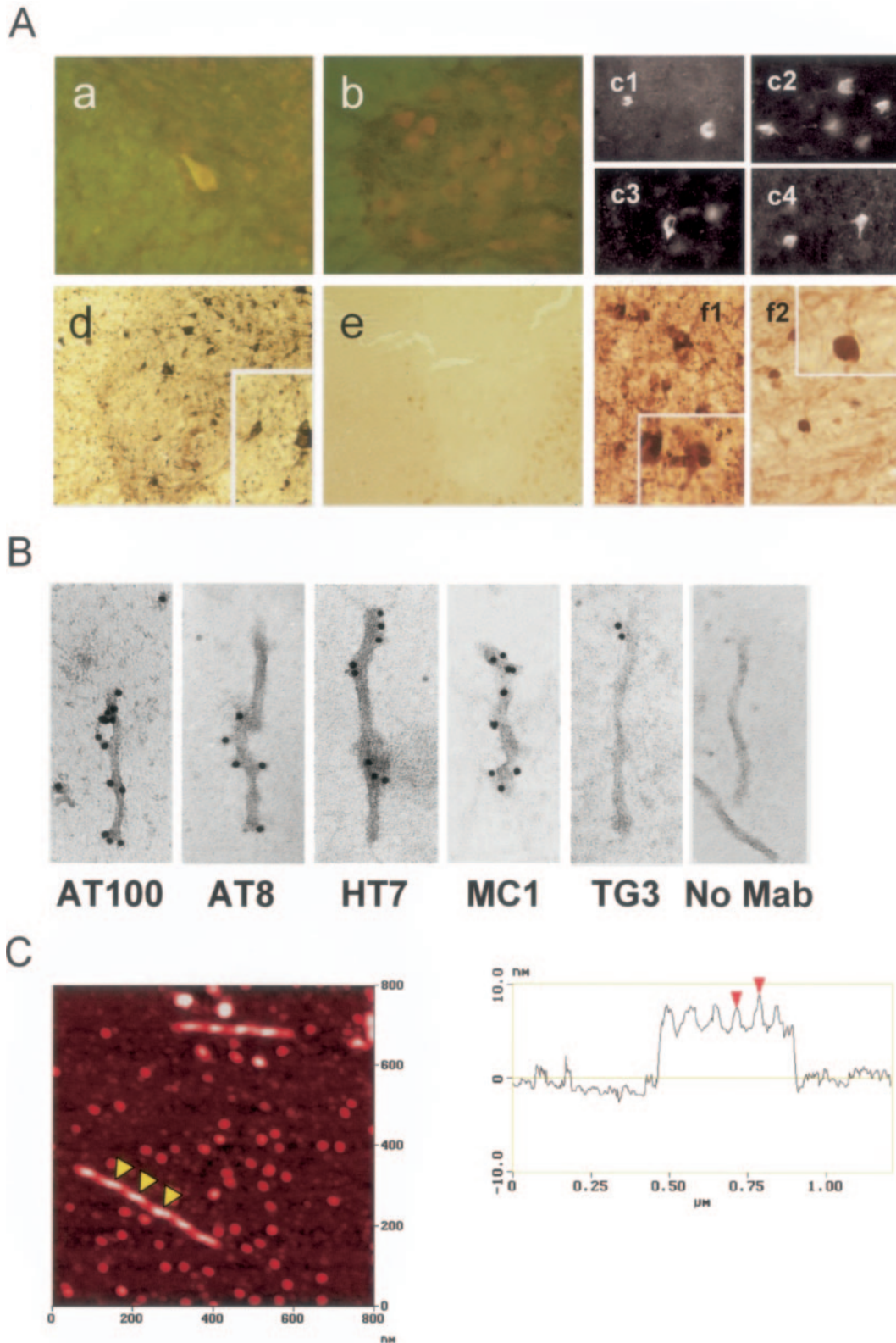


FIG. 6. Tauopathy in old tau-P301L mice. *A*, thioflavin S staining of spinal cord of old tau-P301L mouse (*a*) and tau-4R/2N mouse (*b*). *c1-c4*, staining with X-34 of neurons in brain stem of tau-P301L mouse. Gallyas silver impregnation of spinal cord of tau-P301L mouse (*d*) and nontransgenic mouse (*e*) is shown. Higher magnification (*d*, *inset*) demonstrates argyrophilic grains in dendrites of tau-P301L mouse. *f1*, granular degeneration in neurites in brain stem of tau-P301L mouse visualized with AT8. Note also globular structures in neuronal somata (*inset*, higher magnification). *f2*, axonal dilatations (*inset*, higher magnification) in brain stem of age-matched tau-4R/2N mouse visualized with AT8 (see also Ref. 16). Images and sections are representative of 3–6 mice analyzed for each genotype at 9–12 months of age. *Images a, b, c1-c4, d, and e* are coronal, and *f1-f2* are sagittal. Original magnification was $\times 40$ for *a, b*, and *c1-c4* and $\times 20$ for *d, e*, and *f1-f2*. *B*, tau filaments isolated from old tau-P301L mouse labeled by immunogold (10-nm particles) with primary antibodies as indicated. The filaments are 15–20 nm wide. *C*, tau filaments isolated from old tau-P301L mouse imaged by atomic force microscopy (*left*) with height distribution (*right*) along the longitudinal axis of the filament indicated by the *arrowheads*. The periodicity of the filaments is 60–70 nm, with the height of tops about 9 nm and valleys about 7 nm.

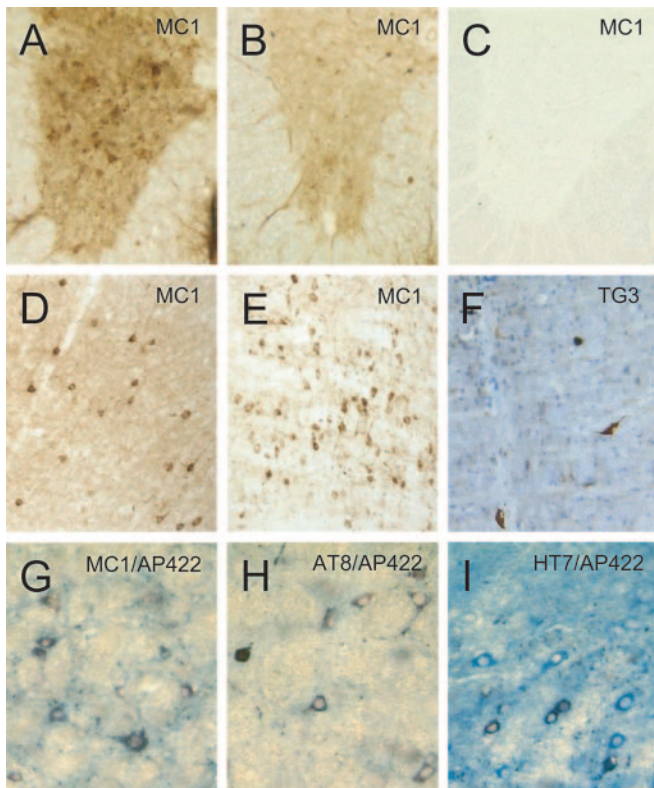


FIG. 7. Conformational tau epitopes in tau-P301L mice and co-localization with phosphorylation epitopes. Immunohistochemistry with MC1 demonstrates immunoreactive neurons in spinal cord (A), brain cortex (D), and midbrain (E) of tau-P301L mice (A, D, and E) but not in tau-4R/2N mice (B) and nontransgenic mice (C). F, TG3-immunoreactive neurons in the coronal section of the brain stem of a 9-month-old tau-P301L mouse. Shown is double immunostaining MC1/AP422 (G) and AT8/AP422 (H) and HT7/AP422 (I). The substrates for staining with AP422 (rabbit polyclonal antibody) produced a red precipitate, whereas staining with mAbs MC1, HT7, and AT8 produced a blue precipitate, resulting in a purple mixed color when co-localized. All mice were 9 months of age. The section used for F was counterstained with hematoxylin. Original magnification was $\times 20$ for A–F and $\times 40$ for G–I.

rabbit polyclonal antibody AP422 and the mAbs MC1, AT8, AT100, or HT7. Essentially, AP422 reacted with the same neurons as MC1, AT100, and AT8 in subcortical areas (Fig. 7, G and H), whereas HT7 evidently stained more neurons in all brain regions (Fig. 7I).

The demonstrated co-localization of MC1 with AP422 can therefore be extended to AT100 and AT8. We conclude from these data that the conformational change of tau defined by MC1 is mechanistically closely related to hyperphosphorylation defined by AT100 and AT8 and to the aggregation process, since all three characteristics are confined to the same neurons.

Some neurons, located mainly in brain stem and spinal cord of old tau-P301L mice, reacted also with TG3 and appeared shrunken and irregular with an eccentrically placed nucleus, resembling ghosts or tomb neurons, since hematoxylin counterstaining did not reveal nuclei (Fig. 7F).

Tau filaments isolated from old tau-P301L mice were ultrastructurally defined as filaments of 10–20-nm width and were straight or twisted (Fig. 6B). The filaments were immunogold-labeled with primary antibodies AT100, AT8, and HT7 and also with MC1 and TG3, demonstrating that the filaments contained conformationally altered hyperphosphorylated tau. Atomic force microscopy demonstrated these tau filaments to be more regular than observed by electron microscopy (Fig. 6C). They appeared as left-handed helical structures with a periodicity of 60–70 nm. Height measurements along the longitudi-

nal axis of a filament revealed peaks of ~ 9 nm and valleys of ~ 7 nm (Fig. 6C). All filamentous structures on the silicon surface displayed very similar characteristics, except for their apparent difference in length.

The combined data are strongly indicative of the close association of hyperphosphorylation, conformational change, and fibril formation in neurons located throughout the CNS, which underlie the neurodegeneration and the moribund tauopathy of tau-P301L mice. All of these characteristics were absent in all tau-4R/2N and tau-KOKI mice analyzed at all ages, indicating that the P301L mutation procured a direct pathological trait not present on or acquired by tau-4R/2N in transgenic mouse brain.

DISCUSSION

We compared three transgenic mouse strains that express the longest isoform of human protein tau (*i.e.* tau-4R/2N with four microtubule binding domains and two N-terminal inserts) (39). Tau-4R/2N mice develop axonopathy with axonal dilations (spheroids) originating from inhibition of axonal transport due to excessive binding of tau-4R/2N to microtubules (16, 32). Two new strains were generated (*i.e.* tau-P301L mice that carry the FTDP-17 mutant P301L in the tau-4R/2N isoform and tau-KOKI mice that express none of the mouse tau isoforms and only human tau-4R/2N at levels similar to endogenous tau levels in wild-type mice).

Importantly, the three transgenic mouse strains express the same tau-4R/2N isoform, all driven by the same murine *thy1* gene promoter and in the same genetic background. Moreover, we selected the tau-P301L strain carefully to express mutant tau-P301L at the same level as tau-4R/2N, leaving the mutation P301L as the only difference. This strict transgenic approach combined with standardized analytical methods applied to these three strains was implemented to obviate any potential controversy from differences in intrinsic parameters or methods.

Major Phenotypic Parameters of Tau-4R/2N, Tau-P301L, and Tau-KOKI Mice—The dramatic differences in phenotype between tau-4R/2N and tau-P301L mice are summarized in Table II. Tau-4R/2N mice have early motor impairment and axonopathy without tau aggregation, as opposed to late and morbid neurofibrillary tauopathy in tau-P301L mice with late but minor motor problems. The gene-dosage effect in tau-4R/2N versus tau-KOKI mice provides considerable information on the mechanism involved.

Tau-KOKI mice were inconspicuous in most phenotypic aspects, with normal embryonic and postnatal development, despite complete absence of tau until the second postnatal week, characteristic for the *thy1* gene promoter used (27, 40). Their motor impairment is minor but clearly demonstrates that even at normal levels, human tau-4R/2N has a much stronger impact on motor ability than mutant tau-P301L. This results in, and is dramatically illustrated by, the severe early motor impairment in the tau-4R/2N mice that correlates closely with the widespread occurrence of axonal dilations or spheroids in all CNS regions (16).

Significantly, despite similar expression levels of tau-P301L and tau-4R/2N, no axonal dilations were observed in tau-P301L mice at any age, not even when terminally ill by the extensive tauopathy. Even more significant is the observation that tau-4R/2N, either at high levels or at normal levels in the absence of murine tau in the tau-KOKI mice, did not produce aggregates. This differs from transgenic mice that overexpress the human tau gene in a murine tau knock-out background (41). In these mice, the tau-3R isoforms accumulate, implying that a shift in tau isoforms and the absence of mouse tau-4R isoforms are the more important parameters in that model.

TABLE II
Phenotypic characteristics of the tau-4R/2N transgenic mice

The level of expression and the severity of the specified phenotypic traits are represented by a proportional number of signs (*i.e.* low (+), moderate (++) , and severe (+++)). The equal sign denotes that the level is similar to endogenous mouse tau with all isoforms combined.

	Tau-4R-KOKI	Tau-4R	Tau-4R-P301L
Expression level	=	+++	+++
Clasping	Normal	+++	+
Rotarod	+	+++	Normal
Beam walk	+, >6 months	+++ , <3 months	+, >9 months
Axonal dilatations	Absent	+++	Absent
Tau aggregates	Absent	Absent	+++
Mean life span	>24 months	>24 months	<12 months

The demonstration that axonal pathology and somal tau pathology can occur independently evidently does not exclude their combination as seen in patients (9) and in transgenic models (25, 42). Significantly, the careful selection for expression and genetic background allowed us to study parameters that mediate axonopathy in tau-4R/2N mice as opposed to tauopathy in tau-P301L mice (*i.e.* hyper-phosphorylation, conformational changes, somato-dendritic relocation, and aggregation), as discussed below.

Tauopathy in Tau-P301L Mice—The pathology in our tau-P301L mice is similar to that in other mutant tau mice (20–22, 25, 42) and is therefore not discussed in depth, except for three important aspects.

Neurons of old tau-P301L mice contained numerous granular deposits that were argyrophilic and marked by pathological tau epitopes. Similar lesions, identified as either small neuropil threads or as argyrophilic grains, are encountered together in AD and in fronto-temporal dementia, whereas argyrophilic grain disease was recently classified as a sporadic tau-4R disease (43, 44). The grains were mainly dendritic in tau-P301L mice but were also evident in ascending axons in the cerebellum, despite very low expression of the transgene in the cerebellum. This aspect deserves further characterization, which falls outside the current study.

Tau filaments isolated from the tau-P301L mice are left-handed helical structures with a regular periodicity and resemble paired helical filaments in AD (45, 46). The filaments were, however, only 9 nm high *versus* a reported 16 nm for paired helical filaments (46), which could be due to differences in tau isoform composition in AD, whereas such detailed information on filaments isolated from the brains of fronto-temporal dementia patients is, to our knowledge, not available.

Mechanistically most important is the intimate occurrence of hyperphosphorylation, conformational change(s), somato-dendritic accumulation, and aggregation in the tau-P301L mice, not seen in the tau-4R/2N mice. The reason why tau-4R/2N does not convert from its evident hyperphosphorylated state into the conformation that allows aggregates to form is unknown, but it could be due to binding to microtubules (see below). The observations on the P301L mutant mice demonstrate that mouse brain neurons are fully capable of forming tau aggregates and tangles, and consequently no essential kinase nor other factor(s) appear to be missing in mouse neurons, including the mechanism responsible for relocation of tau to the soma. The crucial modification of tau-P301L that tau-4R/2N resists or has too high an energy barrier in mouse brain, which is postulated as the decisive parameter, is probably also active in healthy neurons and needs to be identified. The current models with their polarized pathology are believed to be very informative in this respect.

Molecular Differences of Tau-4R/2N and Tau-P301L: Mechanistic Implications—The compartmental (axon *versus* soma) and temporal (early *versus* late) separation of pathology between the tau-4R/2N and tau-P301L transgenic mice is pro-

posed to reflect intrinsic molecular characteristics between the types of tau expressed. Fundamentally, we can explain the observations in terms of the only known molecular action of tau (*i.e.* its binding to microtubules). The axonopathy and motor problems in tau-4R/2N mice result from inhibition of axonal transport by excessive binding of tau-4R/2N to microtubules, driven by mass action (overexpression) and high affinity of tau-4R/2N for microtubules (16–18). Phosphorylation of tau-4R/2N by GSK-3 β , particularly although not exclusively at Ser³⁹⁶/Ser⁴⁰⁴ (AD2 epitope), decreased the binding of tau to microtubules and corrected the axonopathy (17). Additional evidence is provided here by the gene-dosage effect of tau-KOKI *versus* tau-4R/2N mice; due to the lower levels of tau-4R/2N in tau-KOKI mice, less is bound to microtubules, resulting in lesser motor deficits later in life and without axonal swellings (Table I). Conversely, the complete absence of axonal dilatations and the mild and late motor problems in tau-P301L mice is taken as the *in vivo* demonstration that mutant tau-P301L binds less to microtubules, as observed *in vitro* for this (37) and other missense tau mutants (9).

Another conspicuous molecular difference between tau-P301L and tau-4R/2N is in their phosphorylation state (*i.e.* tau-P301L was overall less phosphorylated than tau-4R/2N). This could eventually increase the binding affinity of tau-P301L for microtubules, although we could not find indications that decreased phosphorylation is actually effective as a mechanism to overcome the effect of the mutation (*i.e.* reduced binding to microtubules).

Molecular Differences of Tau-4R/2N and Tau-P301L: Conformation Makes the Difference—The prevailing hypothesis states that tau filaments are formed by increased phosphorylation, releasing tau from the microtubules to increase the pool of unbound phosphorylated tau that aggregates spontaneously. If hyperphosphorylation was the initial trigger of filament formation, this should be reflected in the total pool of tau. However, only a fraction of tau-P301L became hyperphosphorylated with age, whereas overall, tau-P301L remained less phosphorylated than tau-4R/2N. Moreover, in tau-4R/2N transgenic mice, in tau-4R/2N \times GSK-3 β double transgenic mice and in tau-4R/2N \times cdk5 \times p35 triple transgenic mice, we did not detect tau aggregates, despite large intracellular pools of hyperphosphorylated tau (this study) (16, 17, 47) (results not shown). Overexpression of different isoforms or mutants of tau in cells *in vitro*, in combination with various kinases or stimulatory treatments, has not yielded, as yet, a cellular model with filamentous tau aggregation, indicating that factors other than overexpression and hyperphosphorylation are involved, probably with conformational changes as intermediate.

The current study identifies *in vivo* the potentially most decisive differential aspect (*i.e.* the conformational change of tau-P301L, but not of tau-4R/2N). The conformation of tau defined by antibody MC1 highlights the transition from soluble to aggregated filamentous tau, proposed to precede the formation of neurofibrillary tangles (38). Conformational changes

and aggregation of tau in brains of transgenic mice has not, to our knowledge, been demonstrated in the same mice or study. In some tau transgenic mice, the same epitope defined by Alz50 was observed in a limited number of neurons that contained no tau aggregates (16, 48, 49). The strong somatodendritic reaction with MC1 in tau-P301L mice is completely absent in tau-4R/2N and tau-KOKI mice. Moreover, MC1-positive neurons are spatially and temporally closely related to neurons that contain the AT100 and AP422 pathological phosphoepitopes typical for AD and fronto-temporal dementia. Interestingly, the AT100 epitope is formed by phosphorylation of Thr²¹² and Ser²¹⁴ *in vitro* only after induction of conformational changes by polyanions (50), whereas polyanions also induce an intermediate state during filament formation of tau *in vitro* (51). Moreover, the conformational change might render tau in turn a better substrate for other kinases (52). These *in vitro* studies are corroborated here *in vivo* by the intimate correlation of phosphorylation, conformation, and aggregation.

We conclude from our data in combination with published data, as discussed, that an as yet unspecified modification or interaction of tau is responsible for the conformational change that is the necessary intermediate for further phosphorylation and aggregation. Wild-type tau-4R/2N appears to resist this modification, preventing a change in conformation and thereby aggregation. The molecular mechanism needs to be further explored in mice that constitute excellent models for this purpose. Subsequent analysis in diseased and aged human brain will eventually explain the aggregation of tau in tauopathies in which not mutant but wild-type tau is centrally involved.

Acknowledgments—We thank H. Hirokawa, P. Davies, A. Delacourte, and W. Klunk for generous gifts of reagents and for advice. We thank K. Spittaels, C. Van den Haute, L. Umans, L. Serneels, F. Paulussen, H. Geerts, and many others for advice and technical support.

REFERENCES

- Goedert, M. (1996) *Ann. N. Y. Rev. Sci.* **777**, 121–131
- Buée, L., Bussièrè, T., Buée-Scherrer, V., Delacourte, A., and Hof, P. R. (2000) *Brain Res. Rev.* **33**, 95–130
- Lee, V. M., Goedert, M., and Trojanowski, J. Q. (2001) *Annu. Rev. Neurosci.* **24**, 1121–1159
- Larcher, J. C., Boucher, D., Ginzburg, I., Gros, F., and Denoulet, P. (1992) *Dev. Biol.* **154**, 195–204
- Andorfer, C. A., and Davies, P. (2000) *Dev. Neurosci.* **22**, 303–309
- Terwel, D., Dewachter, I., and Van Leuven, F. (2002) *Neuromol. Med.* **2**, 151–165
- Delacourte, A., and Buée, L. (2000) *Curr. Opin. Neurol.* **13**, 371–376
- Heutink, P. (2000) *Hum. Mol. Genet.* **9**, 979–986
- Ingram, E. M., and Spillantini, M. G. (2002) *Trends Mol. Med.* **8**, 555–562
- Wang, J. Z., Gong, C. X., Zaidi, T., Grundke-Iqbal, I., and Iqbal, K. (1995) *J. Biol. Chem.* **270**, 4854–4860
- Friedhoff, P., Schneider, A., Mandelkow, E. M., and Mandelkow, E. (1998) *Biochemistry* **37**, 10223–10230
- Barghorn, S., Zheng-Fischhöfer, Q., Ackmann, M., Biernat, J., von Bergen, M., Mandelkow, E. M., and Mandelkow, E. (2000) *Biochemistry* **39**, 11714–11721
- Alonso, A. C., Zaidi, T., Novak, M., Grundke-Iqbal, I., and Iqbal, K. (2001) *Proc. Acad. Sci. U. S. A.* **98**, 6923–6928
- Gamblin, T. C., Berry, R. W., and Binder, L. I. (2003) *Biochemistry* **42**, 15009–15017
- Gotz, J., Streffer, J., David, D., Schild, A., Hoernli, F., Pennanen, L., Kurosinski, P., and Chen, F. (2004) *Mol. Psychiatry* **7**, 664–683
- Spittaels, K., Van den Haute, C., Van Dorpe, J., Bruynseels, K., Vandezande, K., Laenen, I., Geerts, H., Mercken, M., Sciot, R., Van Lommel, A., Loos, R., and Van Leuven, F. (1999) *Am. J. Pathol.* **155**, 2153–2165
- Spittaels, K., Van den Haute, C., Van Dorpe, J., Geerts, H., Mercken, M., Bruynseels, K., Lasrado, R., Vandezande, K., Laenen, I., Boon, T., Van Lint, J., Vandenhede, J., Moechars, D., Loos, R., and Van Leuven, F. (2000) *J. Biol. Chem.* **275**, 41340–41349
- Mandelkow, E. M., Stamer, K., Vogel, R., Thies, E., and Mandelkow, E. (2003) *Neurobiol. Aging* **8**, 1079–1085
- Hutton, M., Lewis, J., Dickson, D., Yen, S. H., and McGowan, E. (2001) *Trends Mol. Med.* **7**, 467–470
- Lewis, J., McGowan, E., Rockwood, J., Melrose, H., Nacharaju, P., Van Slegtenhorst, M., Gwinn-Hardy, K., Murphy, M. P., Baker, M., Yu, X., Duff, K., Hardy, J., Corral, A., Lin, W. L., Yen, S. H., Dickson, D. W., Davies, P., and Hutton, M. (2000) *Nat. Genet.* **25**, 402–405
- Götz, J., Chen, F., Barmettler, R., and Nitsch, R. M. (2001) *J. Biol. Chem.* **276**, 529–534
- Allen, B., Ingram, E., Takao, M., Smith, M. J., Jakes, R., Virdee, K., Yoshida, H., Holzer, M., Craxton, M., Emson, P. C., Atzori, C., Mighele, A., Crowther, R. A., Ghetti, B., Spillantini, M. G., and Goedert, M. (2002) *J. Neurosci.* **22**, 9340–9351
- Braak, H., and Braak, E. (1991) *Acta Neuropathol.* **82**, 239–259
- Van Leuven, F. (2000) *Prog. Neurobiol.* **61**, 305–312
- Lewis, J., Dickson, D. W., Lin, W. L., Chisholm, L., Corral, A., Jones, G., Yen, S. H., Sahara, N., Skipper, L., Yager, Eckman, C., Hardy, J., Hutton, M., and McGowan, E. (2001) *Science* **293**, 1487–1491
- Oddo, S., Caccamo, A., Shepherd, J. D., Murphy, M. P., Golde, T. E., Kaye, R., Metherate, R., Mattson, M. P., Akbari, Y., and LaFerla, F. M. (2003) *Neuron* **39**, 409–421
- Moechars, D., Lorent, K., De Strooper, B., Dewachter, I., and Van Leuven, F. (1996) *EMBO J.* **15**, 1265–1274
- Chapman, P. F., White, G. L., Jones, M. W., Cooper-Blacketer, D., Marshall, V. J., Irizarry, M., Younkin, L., Good, M. A., Bliss, T. V., Hyman, B. T., Younkin, S. G., and Hsiao, K. K. (1999) *Nat. Neurosci.* **2**, 271–276
- Fitzjohn, S. M., Morton, R. A., Kuenzi, F., Rosahl, T. W., Shearman, M., Lewis, H., Smith, D., Reynolds, D. S., Davies, C. H., Collingridge, G. L., and Seabrook, G. R. (2001) *J. Neurosci.* **21**, 4691–4698
- Ris, L., Dewachter, I., Reverse, D., Godaux, E., and Van Leuven, F. (2003) *J. Biol. Chem.* **278**, 44393–44399
- Gureviciene, I., Ikonen, S., Gurevicius, K., Sarkaki, A., van Groen, T., Pussinen, R., Ylinen, H., and Tanila, H. (2004) *Neurobiol. Dis.* **15**, 188–195
- Kunzi, V., Glatzel, M., Nakano, M. Y., Greber, U. F., Van Leuven, F., and Aguzzi, A. (2002) *J. Neurosci.* **22**, 7471–7477
- Harada, A., Oguchi, K., Okabe, S., Kuno, J., Terada, S., Oshima, T., Sato-Yoshitake, R., Takei, Y., Noda, T., and Hirokawa, N. (1994) *Nature* **369**, 488–491
- Umans, L., Serneels, L., Overbergh, L., Lorent, K., Van Leuven, F., and Van den Berghe, H. (1995) *J. Biol. Chem.* **270**, 19778–19785
- Gallyas, F. (1971) *Acta Morphol. Acad. Sci. Hung.* **19**, 1–8
- Styren, S. D., Hamilton, R. L., Styren, G. C., and Klunk, W. E. (2000) *J. Histochem. Cytochem.* **48**, 1223–1232
- Hong, M., Zhukareva, V., Vogelsberg-Ragaglia, V., Wszolek, Z., Reed, L., Miller, B. I., Geschwind, D. H., Bird, T. D., McKeel, D., Goate, A., Morris, J. C., Wilhelmsen, K. C., Schellenberg, G. D., Trojanowski, J. Q., and Lee, V. M. (1998) *Science* **282**, 1914–1917
- Weaver, C. L., Espinoza, M., Kress, Y., and Davies, P. (2000) *Neurobiol. Aging* **21**, 719–727
- Goedert, M., Spillantini, M., Potier, M., Ulrich, J., and Crowther, R. (1989) *EMBO J.* **82**, 393–399
- Dewachter, I., Reverse, D., Caluwaerts, N., Ris, L., Kuiperi, C., Van den Haute, C., Spittaels, K., Umans, L., Serneels, L., Thiry, E., Moechars, D., Mercken, M., Godaux, E., and Van Leuven, F. (2002) *J. Neurosci.* **22**, 3445–3453
- Andorfer, C., Kress, Y., Espinoza, M., de Silva, R., Tucker, K. L., Barde, Y. A., Duff, K., and Davies, P. (2003) *J. Neurochem.* **86**, 582–596
- Lin, W. L., Lewis, J., Yen, S. H., Hutton, M., and Dickson, D. W. (2003) *Am. J. Pathol.* **162**, 213–218
- Tolnay, M., Mistl, C., Ipsen, S., and Probst, A. (1998) *Neuropathol. Appl. Neurobiol.* **24**, 53–59
- Togo, T., Sahara, N., Yen, S., Cookson, N., Ishiwaza, T., Hutton, M., de Silva, R., Lees, A., and Dickson, D. W. (2002) *J. Neuropathol. Exp. Neurol.* **61**, 547–556
- Crowther, R. A., and Wischik, C. M. (1985) *EMBO J.* **4**, 3661–3665
- Moreno-Herrero, F., Pérez, M., Baro, A. M., and Avila, J. (2004) *Biophys. J.* **86**, 517–525
- Van den Haute, C., Spittaels, K., Van Dorpe, J., Lasrado, R., Vandezande, K., Laenen, I., Geerts, H., and Van Leuven, F. (2001) *Neurobiol. Dis.* **1**, 32–44
- Brion, J. P., Tremp, G., and Octave, J. N. (1999) *Am. J. Pathol.* **154**, 255–270
- Ishihara, T., Hong, M., Zhang, B., Nakagawa, Y., Lee, M. K., Trojanowski, J. Q., and Lee, V. M. (1999) *Neuron* **24**, 751–762
- Zheng-Fischhöfer, Q., Biernat, J., Mandelkow, E. M., Illenberger, S., Godemann, R., and Mandelkow, E. (1998) *Eur. J. Biochem.* **252**, 542–552
- Chirita, C. N., and Kuret, J. (2004) *Biochemistry* **43**, 1704–17014
- Hasegawa, M., Crowther, R. A., Jakes, R., and Goedert, M. (1997) *J. Biol. Chem.* **272**, 33118–33124
- Mercken, M., Vandermeeren, M., Lubke, U., Six, J., Boons, J., Van Mechelen, E., Van de Voorde, A., and Gheuens, J. (1992) *J. Neurochem.* **58**, 548–553
- Riederer, B., and Binder, L. (1994) *Brain Res. Bull.* **2**, 155–161
- Goedert, M., Jakes, R., and Vanmechelen, E. (1995) *Neurosci Lett* **189**, 167–169
- Goedert, M., Jakes, R., Crowther, R. A., Cohen, P., Vanmechelen, E., Vandermeeren, M., and Cras, P. (1994) *Biochem. J.* **301**, 871–877
- Buée-Scherrer, V., Condamines, O., Mourton-Gilles, C., Jakes, R., Goedert, M., Pau, B., and Delacourte, A. (1996) *Mol. Brain Res.* **39**, 79–88
- Caillet-Boudin, M. L., and Delacourte, A. (1996) *NeuroReport* **8**, 307–310
- Jicha, G. A., Lane, E., Vincent, I., Otvos, L., Jr., Hoffmann, R., and Davies, P. (1997) *J. Neurochem.* **69**, 2087–2095